Comparative Medicine
Copyright 2024
by the American Association for Laboratory Animal Science

Vol 74, No 2
April 2024
Pages 121–129

Chlamydia muridarum Associated Pulmonary and Urogenital Disease and Pathology in a Colony of Enzootically Infected Il12rb2 Deficient and Stat1 Knockout Mice

Noah Mishkin, DVM,[1,*] Ileana C Miranda, DVM, MSc, DACVP,[1,2] Sebastian E Carrasco, DVM, MPVM, MSc, PhD, DACVP,[1,2] Christopher Cheleuitte-Nieves, PhD, DVM, DACLAM,[1,2] Rodolfo J Ricart Arbona, MLAS, DVM, DACLAM,[1,2] Claire Wingert, BA,[3] Joseph C Sun, PhD,[3] and Neil S Lipman, VMD, DACLAM[1,2,*]

***Chlamydia muridarum* (Cm), an intracellular bacterium of historical importance, was recently rediscovered as moderately prevalent in research mouse colonies. Cm was first reported as a causative agent of severe pneumonia in mice about 80 y ago, and while it has been used experimentally to model *Chlamydia trachomatis* infection of humans, there have been no further reports of clinical disease associated with natural infection. We observed clinical disease and pathology in 2 genetically engineered mouse (GEM) strains, *Il12rb2*KO and *STAT1*KO, with impaired interferon-γ signaling and Th1 CD4+ T cell responses in a colony of various GEM strains known to be colonized with and shedding Cm. Clinical signs included poor condition, hunched posture, and poor fecundity. Histopathology revealed disseminated Cm with lesions in pulmonary, gastrointestinal, and urogenital tissues. The presence of Cm was confirmed using both immunohistochemistry for Cm major outer membrane protein-1 antigen and in situ hybridization using a target probe directed against select regions of Cm strain Nigg. Cm was also found in association with a urothelial papilloma in one mouse. These cases provide additional support for excluding Cm from research mouse colonies.**

Abbreviations and Acronyms: Cm, *Chlamydia muridarum*; ECP, eosinophilic crystalline pneumonia; GALT, gut-associated lymphoid tissue; GEM, genetically engineered mouse; HE, hematoxylin and eosin; IFU, inclusion-forming units; IHC, immunohistochemistry; *Il12rb2*, beta 2 gene of the interleukin-12 receptor; *Il12rb2*KO, B6.129S1-*Il12rb2*^{tm1Jm}/J; ISH, in situ hybridization; MOMP, major outer membrane protein; MSK, Memorial Sloan Kettering Cancer Center; NSG, NOD.Cg-*Prkdc*^{scid} Il2rg^{tm1Wjl}/SzJ; *STAT1*, signal transducer and activator of transcription 1 gene; *STAT1*KO, B6.129S(Cg)-*Stat1*^{tm1Dlv}/J

DOI: 10.30802/AALAS-CM-24-000002

Introduction

Chlamydia muridarum (Cm) was recently reported as prevalent in research mouse colonies, affecting between 14% and 33% of noncommercial institutions assayed with an intrainstitutional prevalence of around 63%.[28] While the reasons for the high prevalence of this bacterium in academic mouse colonies are unknown, the historic failure to acknowledge and test for its presence along with widespread interinstitutional sharing of genetically engineered mouse (GEM) strains likely had a significant role. Further supporting this organism's ability to 'hide in plain sight' is the observation that infected immunocompetent mouse strains remain subclinical, with infections discovered incidentally during routine colony health surveillance and/or secondary to experimental use.[28,45]

To date, clinical disease has only been observed in mice in association with Cm's initial discovery after serial passage of biologic samples, after experimental infection of mice used to study human Chlamydial infections, or after cohousing of NOD.Cg-*Prkdc*^{scid} Il2rg^{tm1Wjl}/SzJ (NSG) mice with Cm-shedding mice.[28,34] In the initial discoveries made in the late 1930s and early 1940s, severe interstitial pneumonia leading to acute death was observed and attributed to the "mouse pneumonitis virus," which we now know as Cm.[10,13,29] Since this discovery, Cm has been extensively used as a translational model for human *Chlamydia trachomatis* infection. Cm's experimental use generally relies on presumed atypical inoculation routes (primarily urogenital and respiratory rather than gastrointestinal), large infectious doses (often up to or exceeding 10^6 inclusion-forming units [IFUs]), progesterone pretreatment, and/or use of immunocompromised mice.[4,34,35,45] Recent literature indicates that the ID_{50} for experimental gastrointestinal infections of immunocompetent mice may be as low as 10^2 IFUs and result in persistent subclinical colonization.[45] Clinical disease in these translational studies varied based on the route of inoculation, experimental dose, and mouse strain but included respiratory, urogenital, and cardiac disease.[12,35] We recently reported peribronchiolar lymphocytic and plasmocytic aggregates associated

Submitted: 05 Jan 2024. Revision requested: 15 Jan 2024. Accepted: 25 Feb 2024.
[1]Tri-Institutional Training Program in Laboratory Animal Medicine and Science, Memorial Sloan Kettering Cancer Center, Weill Cornell Medicine, and The Rockefeller University, New York, New York; [2]Center of Comparative Medicine and Pathology, Memorial Sloan Kettering Cancer Center and Weill Cornell Medicine, New York, New York; and [3]Program in Immunology, Memorial Sloan Kettering Cancer Center, New York, New York
[*]Corresponding authors. Emails: mishkinn@mskcc.org or lipmann@mskcc.org
This article contains supplemental materials online.

with Cm infection in 2 asymptomatic, immunocompetent GEM mouse strains.[28] Additional investigations demonstrated that NSG mice developed severe clinical disease when cohoused with Cm-shedding mice.[28,38] A considerable subset of NSG mice demonstrated dyspnea, lethargy, weight loss, hunched posture, and unkempt coats within 28 d of exposure. A bronchointerstitial pneumonia characterized by dense neutrophilic and histiocytic infiltrates associated with Cm inclusions in bronchiolar and alveolar epithelial cells was frequently observed in the affected NSG mice. Up to one-third of the mice in this cohort also had endometritis and salpingitis, rhinitis, tracheitis, and/or nasopharyngitis associated with Cm inclusions in mucosal epithelial cells.[28,38]

Herein we report clinical disease and pathology observed spontaneously in 2 GEM strains with impaired interferon-γ (IFN-γ) signaling and Th1 CD4+T cell responses in a colony of various GEM and inbred strains infected with and shedding Cm. This report is the first since the initial discovery of Cm to describe Cm infection leading to clinical disease in mice that had not been experimentally infected with the bacterium. The phenotype of the affected mouse strains reinforces our understanding of the immune response to Cm and highlights the importance of research and veterinary staff recognizing that some GEM strains may be uniquely impacted by Cm infection.

Case Series

Background and clinical presentation. *Il12rb2KO*. These mice are engineered to remove the β-2 gene of the interleukin 12 receptor (IL12rb2). Briefly, B6.129S1-*Il12rb2*^{tm1Jm}/J mice (*Il12rb2*KO) are used in studies of allergy, autoimmune disease, and microbial infections, including *C. trachomatis* and Cm.[19,20,25,44] These mice are used to investigate the role of IL12 and IL12-mediated signals on NK and T cell activation, proliferation, trafficking, and memory formation. Neither the immune status of these nor of the *STAT1*KO mice described below dictated that they required more stringent husbandry standards than provided for immunocompetent strains at our institution. Four experimentally naïve, 1.5-mo-old female mice presented with poor condition and hunched posture, one of which was moribund and therefore immediately euthanized without the option of performing further diagnostics. The remaining 3 mice were confirmed to be Cm positive via fecal PCR and submitted for complete necropsy. Another three 4-mo-old male mice that had no clinical signs were found to be Cm positive based on pooled fecal PCR and also underwent complete necropsy.

STAT1KO. These mice are engineered to remove the signal transducer and activator of transcription 1 (*STAT1*) gene. Briefly, B6.129S(Cg)-*Stat1*^{tm1Dlv}/J mice (*STAT1*KO) are similarly used to study NK and T cell response after microbial infection.[11,26] Deletion of *STAT1* interferes with the regulation of the JAK/STAT1 signaling pathway and renders these mice unable to respond to type 1 and type 2 interferon (IFN) signals (IFNα/β and IFNγ, respectively).[15] These mice are particularly susceptible to infections with viral pathogens and intracellular bacteria, such as *Chlamydia pneumoniae* and Cm.[32,36] Mice from this colony had a recent history of fewer litters per breeding pair, smaller litter sizes, runted pups, increased pup mortality, fur loss, and skin irritation that sometimes persisted into adulthood. A breeding pair of 6.5-mo-old mice was submitted for complete necropsy.

Materials and Methods

Animals. *IL12rb2*KO and *STAT1*KO mice were bred in-house by the research laboratory. Based on findings from the prior year's colony health monitoring, which uses soiled bedding sentinels, these mice were presumed to be free of mouse hepatitis virus, Sendai virus, mouse parvovirus, minute virus of mice, pneumonia virus of mice, Theiler meningoencephalitis virus, mouse rotavirus, murine astrovirus 2, reovirus 3, Ectromelia virus, lymphocytic choriomeningitis virus, K-virus, mouse adenovirus 1 and 2, polyoma virus, rodent chaphamaparvovirus 1, mouse cytomegalovirus, mouse thymic virus, hantavirus, *Mycoplasma pulmonis*, *Filobacterium rodentium* (CAR *Bacillus*), *Clostridium pilliforme*, *Citrobacter rodentium*, *Salmonella* spp., *Klebsiella pneuominae/oxytoca*, *Streptococcus pneumoniae*, *Corynebacterium kutscheri*, *Streptobacillus moniliformis*, *Encephalitozoon cuniculi*, *Giardia muris*, fur mites, and pinworms and were potentially infected with *Helicobacter* spp., segmented filamentous bacteria, *Demodex musculi*, *Spinonucleus muris*, and/or Cm.[23] PCR testing of fecal pellets pooled by cage confirmed a high prevalence of Cm infection of both the *Il12rb2*KO and *STAT1*KO colonies.

Mice were maintained in individually ventilated polysulfone shoebox cages with stainless-steel wire-bar lids and filter tops (number 19, Thoren Caging Systems, Hazelton, PA) on autoclaved aspen chip bedding (PWI Industries, Quebec, Canada) at a density of no greater than 5 mice per cage. Each cage was provided with an autoclaved Glatfelter paper bag containing 6g of crinkled paper strips (EnviroPak, WF Fisher and Son, Branchburg, NJ) for enrichment. Mice were fed a natural ingredient, closed source, flash-autoclaved, γ-irradiated feed (LabDiet 5053, PMI, St. Louis, MO).[40] All mice received reverse osmosis acidified (pH 2.5 to 2.8 with hydrochloric acid) water ad libitum from polyphenylsulfone bottles with stainless-steel caps and sipper tubes (Techniplast, West Chester, PA). Cages were changed every 7 d in a change station (Nuaire NU-S612-400, Nuaire, Plymouth, MN). All cages were located in a room that supported a single laboratory and housed numerous GEM and inbred strains. The room was maintained on a 12:12-h light:dark cycle, relative humidity of 30% to 70%, and room temperature of 72 ± 2 °F (22 ± 1 °C). The animal care and use program at Memorial Sloan Kettering Cancer Center (MSK) is accredited by AAALAC International, and all animals are maintained in accordance with the recommendations provided in the *Guide for the Care and Use of Laboratory Animals*.[19] All investigative animal use was approved by MSK's IACUC in agreement with AALAS' position statements on the Humane Care and Use of Laboratory Animals and Alleviating Pain and Distress in Laboratory Animals.[2,3]

Pathology. After euthanasia by CO_2 asphyxiation, complete necropsies were performed and gross lesions were recorded. All tissues including the heart, thymus, lungs, liver, gallbladder, kidneys, pancreas, stomach, duodenum, jejunum, ileum, cecum, colon, lymph nodes (mandibular, mesenteric), salivary glands, skin (trunk and head), urinary bladder, uterus, cervix, vagina, ovaries, oviducts, testes, epididymides, seminal vesicles, prostate, adrenal glands, spleen, thyroid gland, esophagus, trachea, spinal cord, vertebrae, sternum, femur, tibia, stifle joint, skeletal muscle, nerves, skull, nasal cavity, oral cavity, teeth, ears, eyes, pituitary gland, and brain were fixed in 10% neutral buffered formalin. After fixation, the skull, spinal column, sternum, femur, and tibia were decalcified in a formic acid and formaldehyde solution (Surgipath Decalcifier I,

Leica Biosystems). Tissues were then processed in ethanol and xylene and embedded in paraffin in a tissue processor (Leica ASP6025, Leica Biosystems). Paraffin blocks were sectioned at 5-µm, stained with hematoxylin and eosin (HE), and examined by 1 of 2 American College of Veterinary Pathologists certified veterinary pathologists (SEC for IL12rb2KO and ICM for STAT1KO mice).

Immunohistochemistry. Lungs, gastrointestinal tracts, and urogenital tracts evaluated by histopathology were screened for chlamydial major outer membrane protein (MOMP) using an immunohistochemistry (IHC) method previously validated by MSK's Laboratory of Comparative Pathology.[28,38] Briefly, formalin-fixed paraffin-embedded sections were stained using an automated staining platform (Leica Bond RX, Leica Biosystems). After deparaffinization and heat-induced epitope retrieval in a citrate buffer at pH 6.0, the primary antibody against chlamydial MOMP (NB100-65054, Novus Biologicals, Centennial, CO) was applied at a dilution of 1:500. A rabbit antigoat secondary antibody (cat. no. BA-5000, Vector Laboratories, Burlingame, CA) and a polymer detection system (DS9800, Novocastra Bond Polymer Refine Detection, Leica Biosystems) were then applied to the tissues. The 3,3′-diaminobenzidine tetrachloride was used as the chromogen, and the sections were counterstained with hematoxylin and examined by light microscopy. Reproductive tracts from Toll-like receptor-3-deficient mice that had been experimentally infected with Cm strain Nigg were used as the positive control.

In addition, the bronchiolar and vascular inflammatory cell populations observed in lung tissue were further characterized by IHC. After deparaffinization and heat-induced epitope retrieval as above, antibodies against CD3, CD4, CD8, and B220 were applied, followed by incubation with secondary antibodies and detection. Anti-CD3 (ab136732, Abcam, Waltham, MA; dilution 1:250) used a goat antirabbit secondary antibody (BA-1000 Vector Laboratories, Burlingame, CA), whereas anti-B220 (550286, BD Biosciences, Franklin Lakes, NJ; dilution 1:200), anti-CD4 (14-9766-82, Thermo Fisher Scientific, Waltham, MA; dilution 1:250), and anti-CD8 (14-0808-82, Thermo Fisher Scientific, Waltham, MA; dilution 1:1000) all used a rabbit antirat secondary antibody (BA-4001, Vector Laboratories, Burlingame, CA). Slides were double stained for either CD3/B220 or CD4/CD8. A polymer detection system (PK6100, Vector Laboratories, Burlingame, CA) was then applied to the tissues.

In situ hybridization. Lungs were also evaluated using in situ hybridization (ISH). The target probe was designed to detect regions 581 to 617 of Cm strain Nigg's complete sequence, NCBI Reference Sequence NC_002620.2 (1039538-C1, Advanced Cell Diagnostics, Newark, CA). The target probe was validated on reproductive tracts from mice that had been experimentally infected with Cm strain Nigg. Slides were stained on an automated stainer (Leica Bond RX, Leica Biosystems) with RNAscope 2.5 LS Assay Reagent Kit-Red (322150, Advanced Cell Diagnostics) and Bond Polymer Refine Red Detection (DS9390, Leica Biosystems). Control probes were used to detect a validated positive housekeeping gene (mouse peptidylprolyl isomerase B, Ppib) to confirm adequate RNA preservation and detection (313918, Advanced Cell Diagnostics), and a negative control, *Bacillus subtilis* dihydrodipicolinate reductase gene (dapB) was used to confirm absence of nonspecific staining (312038, Advanced Cell Diagnostics). Positive RNA hybridization was identified as discrete punctate chromogenic red dots under bright field microscopy.

Results

Pathology. *IL12rb2KO.* Macroscopically, the 3 female mice with clinical signs showed poor condition (2/5 body condition score).[41] Lungs were mottled red-to-pink or pink-to-white; one mouse also had pinpoint pale-pink foci of pleural discoloration. Their thymuses were markedly small, and 2 mice had enophthalmos. No gross abnormalities were observed in the 3 clinically normal male mice.

Histologically, 2 of the female mice with clinical signs had a mild to moderate multifocal peribronchiolar and perivascular lymphoplasmahistiocytic bronchopneumonia with bronchiolar epithelial cell degeneration, alveolar histiocytosis, and intralesional Cm inclusions (Figure 1A–C). The lungs from the remaining mouse had a focal lymphohistiocytic bronchiolitis without Cm inclusions. All 3 female mice also had marked generalized thymic hypoplasia with lymphoid hypocellularity. All 3 clinically normal male mice had a minimal typhlocolitis with reactive gut-associated lymphoid tissue (GALT; similar to Figure 2A), and 2 of the 3 male mice also had eosinophilic crystalline pneumonia (ECP); however, Cm inclusions were not observed.

STAT1KO. Macroscopically, mice had good body condition (3/5 body condition score). However, their urinary tracts were abnormal. The male presented with an enlarged left kidney (approximately twice the size of the normal right kidney) that was markedly distended by clear fluid (hydronephrosis), rendering the cortex thin (Figure 3, left). The female presented with a mildly enlarged right and a severely enlarged left kidney (approximately 3 times the size of right); the left kidney was markedly distended by a cloudy tan-to-pale-yellow fluid (pyonephritis), rendering the cortex thin (Figure 3, right). The left renal lymph nodes were also enlarged.

Histologically, the male had severe unilateral (left) hydronephrosis with diffuse parenchymal atrophy and moderate, multifocal to coalescing neutrophilic lymphoplasmahistiocytic pyelonephritis. This mouse also had moderate multifocal neutrophilic lymphoplasmahistiocytic rhinitis and tracheitis with submucosal lymphoid follicular hyperplasia, and moderate, multifocal peribronchiolar and perivascular to interstitial neutrophilic lymphoplasmahistiocytic bronchointerstitial pneumonia (similar to Figure 1A–C, but Cm inclusions were not visualized; full images are shown in Figure S1A and B) with lymphoid follicular hyperplasia of the bronchus-associated lymphoid tissue (BALT) and tracheobronchial lymph nodes (Figure S1A). Other findings in this mouse included minimal, multifocal, neutrophilic gastritis at the limiting ridge with intraepithelial Cm inclusions in gastric mucous cells, minimal to mild, multifocal lymphoplasmacytic enteritis with no visible Cm inclusions, GALT hyperplasia with prominent germinal centers (Figure 2A), and minimal to mild, multifocal, lymphoplasmahistiocytic typhlocolitis with intraepithelial Cm inclusions in surface enterocytes (Figure 2C).

Urogenital lesions in the female included severe pyonephritis (left) with diffuse parenchymal atrophy and multifocal to coalescing, neutrophilic lymphoplasmahistiocytic pyelonephritis, moderate hydronephrosis (right) with locally extensive parenchymal atrophy, medullary and cortical tubular degeneration, and mild, multifocal lymphoplasmahistiocytic interstitial nephritis (Figure 4A–D). A urothelial papilloma was present in the left renal pelvis in association with severe multifocal to coalescing neutrophilic lymphoplasmahistiocytic inflammation with Cm inclusions present in the urothelial cells lining the tumor but not in the cells lining the adjacent renal pelvis (Figure 4E). Severe, diffuse neutrophilic lymphoplasmahistiocytic unilateral

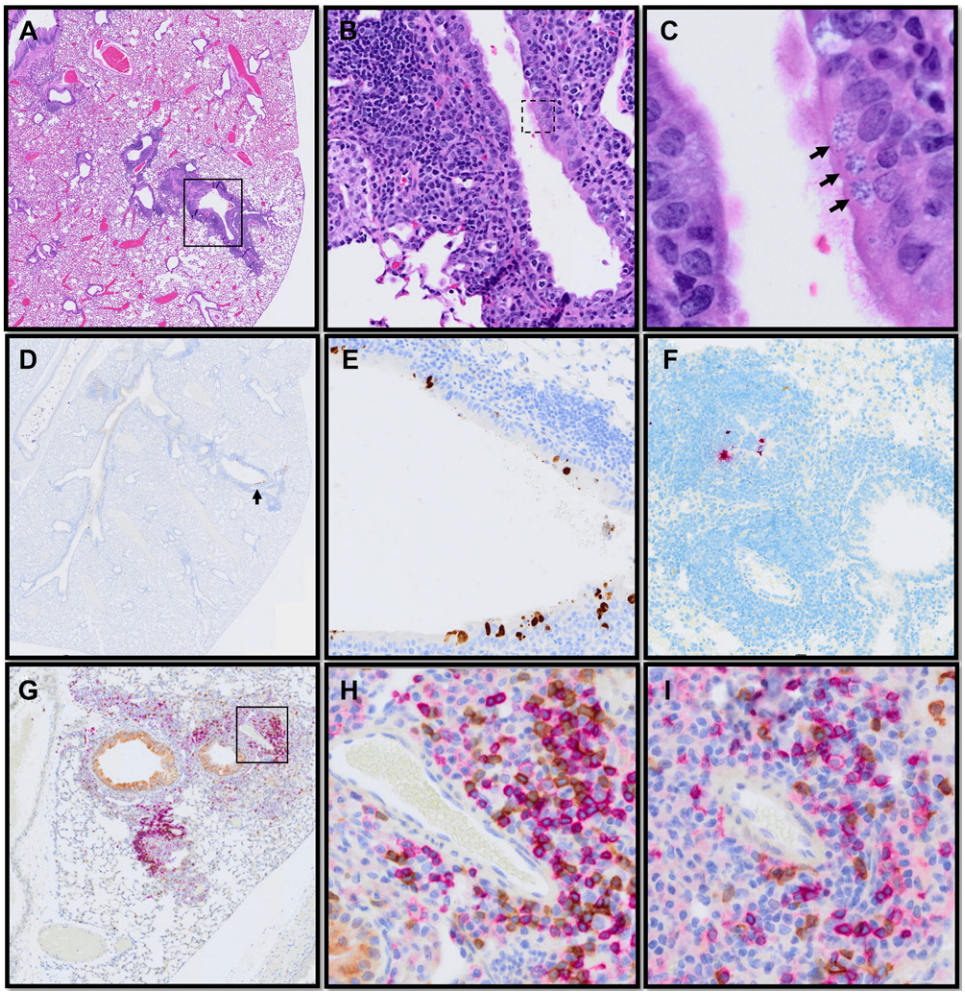

Figure 1. Cm associated bronchopneumonia, lung, *Il12rb2*KO mice. (A) Mild to moderate multifocal peribronchiolar and perivascular bronchopneumonia in a clinically affected female mouse. HE, subgross. (B) Lymphoplasmacytic and histiocytic bronchopneumonia noted boxed in A, with intraepithelial Cm inclusions. HE, 10×. (C) Higher magnification of Cm inclusions noted in hatched box in B (arrows). HE, 40×. (D) Cm signal in bronchiolar epithelial cells within inflammatory lesions noted on HE (arrow, brown staining). IHC for Cm MOMP, subgross. (E) Cm in bronchiolar epithelial cells (brown staining). IHC for Cm MOMP, 10×. (F) Cm nucleic acid in bronchiolar epithelial cell of a clinically normal male *Il12rb2*KO mouse (red staining). ISH for Cm RNA. (G) Peribronchiolar and perivascular T and B cell infiltrates surrounding Cm positive epithelial cells (CD3+ brown, B220+ red). Double staining IHC for CD3 and B220, 2×. (H) Higher magnification of boxed area in G (CD3+ brown, B220+ red). Double staining IHC for CD3 and B220, 20× (I) Further differentiation of subpopulations of CD3+ cells in same area as in H (CD4+ red, CD8+ brown). Double staining IHC for CD4 and CD8, 20×.

(left) ureteritis (Figure 5A) and cystitis (Figure 5B) with intraurothelial Cm inclusions and hyaline droplet accumulation (Figure 5A, inset), occasional urothelial cell necrosis, and adjacent/submucosal lymphoid follicular hyperplasia (Figure 5A and B) were also present. Reproductive tract lesions included severe, unilateral (left), multifocal to coalescing neutrophilic lymphoplasmahistiocytic metritis and salpingitis, and severe unilateral (left) ovarian parenchymal atrophy with a multifocal to coalescing neutrophilic lymphoplasmahistiocytic to granulomatous periovarian steatitis and myositis (Figure 5C). Pulmonary lesions included mild to moderate, multifocal, lymphoplasmacytic rhinitis and tracheitis, and moderate, multifocal, peribronchiolovascular to interstitial neutrophilic lymphoplasmahistiocytic bronchointerstitial pneumonia with intraepithelial Cm inclusions (similar to Figure 1A–C; full images shown in Figure S1D and E) and BALT and tracheobronchial lymph node hyperplasia. Gastrointestinal lesions included minimal, multifocal, neutrophilic gastritis at the limiting ridge with intraepithelial Cm inclusions in gastric mucous cells and minimal to mild, multifocal, neutrophilic lymphoplasmahistiocytic enteritis, typhlitis, and colitis with intraepithelial Cm inclusions (cecum and colon) and surface cecal enterocytes necrosis (similar to Figure 2C). Other findings in this mouse included moderate to severe, multifocal to coalescing, neutrophilic lymphoplasmahistiocytic to granulomatous peritonitis, and moderate to severe multifocal proliferative and necrotizing neutrophilic arteritis with intimal fibrinoid necrosis and adventitial hyperplasia.

IHC and ISH. *IL12rb2KO*. In the 3 female mice with clinical signs, strong, specific Cm MOMP-1 antigen immunolabeling was observed in bronchiolar epithelial cells in association with the inflammatory lesions (Figure 1D–E). Antigen was also detected in small and large intestinal surface epithelial cells of all 3 mice (Figure 2B, inset). All 3 male mice had strong, specific Cm MOMP-1 antigen staining throughout the surface cecal and colonic epithelium. Two of these 3 mice also showed rare but strong and specific staining of bronchiolar epithelial cells.

Additional IHC was performed on the lung of a female mouse to assess the major lymphoid subsets in pulmonary lesions. The perivascular and peribronchiolar inflammatory populations were comprised of multifocal clusters of B and T cells, depicted by B220 and CD3 immunolabeling, respectively.

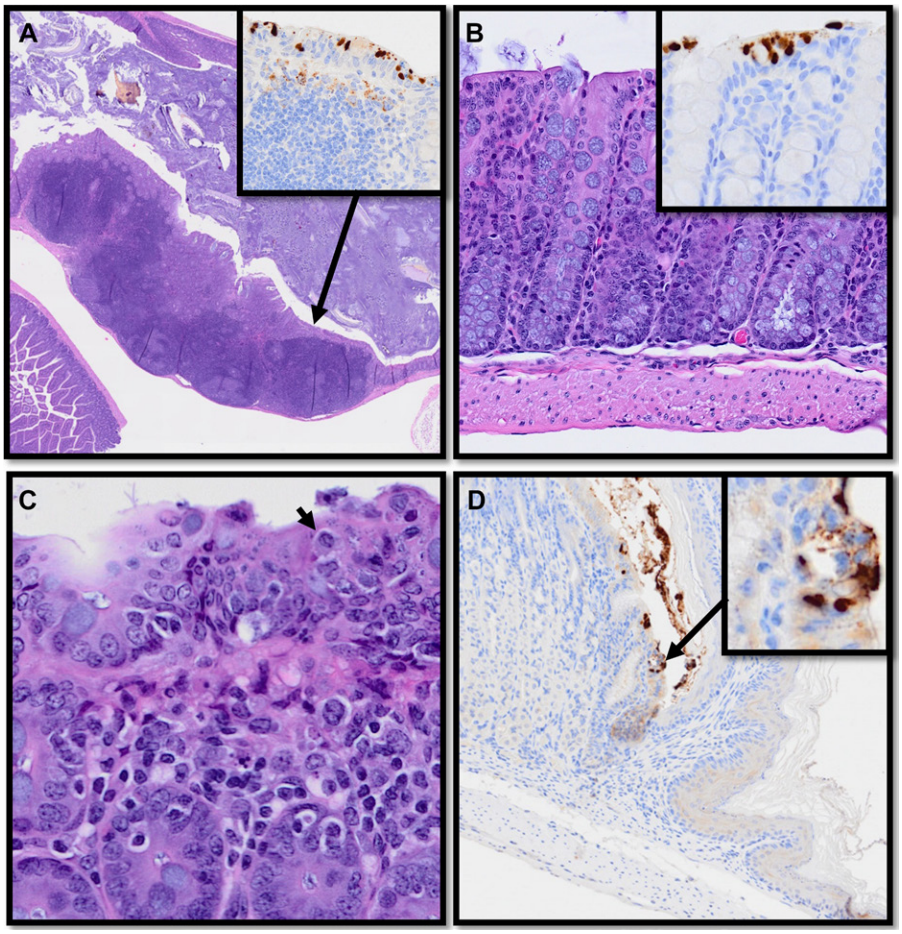

Figure 2. Reactive GALT hyperplasia and Cm colonization in the gastrointestinal tract. (A) GALT hyperplasia with prominent germinal centers, cecum, male *STAT1*KO mouse. HE, subgross. Inset: Cm signal in surface cecal epithelial cells (brown staining). IHC for Cm MOMP, 10×. (B) Histologically normal colon from a clinically affected female *Il12rb2*KO mouse. HE, 10×. Inset: Cm signal in surface colonic epithelial cells (brown staining). IHC for Cm MOMP, 10×. (C) Male *STAT1*KO mouse, minimal to mild lymphoplasmacytic, histiocytic, and neutrophilic typhlitis, with Cm inclusion (arrow), cecum. HE, 20×. (D) Female *STAT1*KO mouse, Cm signal within surface epithelial cells at the gastric limiting ridge (brown staining). IHC for Cm MOMP, 4×.

CD4 and CD8 positive cells (Figure 1G–I) were observed frequently in areas with peribronchiolovascular inflammation.

ISH signal was detected in association with the peribronchiolovascular inflammation in the 2 clinically normal male mice in which Cm nucleic acid was sporadically detected in bronchiolar epithelial cells (Figure 1F).

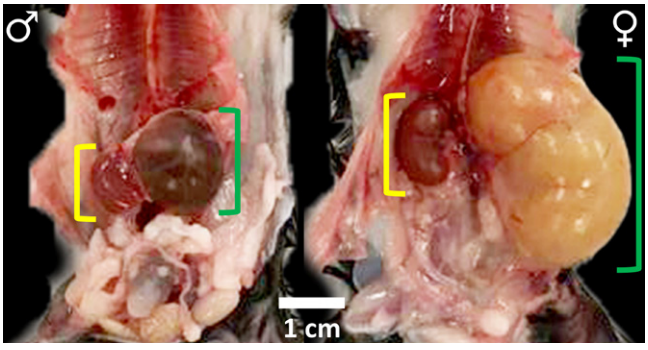

Figure 3. Macroscopic changes in the kidneys of *STAT1*KO mice infected with Cm. Male mouse (left) presented with a markedly enlarged left kidney (small green bar) approximately 2× normal size (for example right kidney, small yellow bar). Female mouse (right) presented with mildly enlarged right kidney (larger yellow bar) and markedly enlarged left kidney (larger green bar) (approximately 3× the size of the contralateral kidney).

STAT1KO. Strong specific staining for Cm MOMP-1 antigen was observed in numerous tissues, including surface epithelial cells throughout the small intestine, cecum, and colon, mucous cells at the gastric limiting ridge of both mice (female mouse depicted in Figure 2D), and bronchiolar epithelial cells (Figure S1F) of the female mouse. Strong IHC signal was also detected in the urothelial cells of the papilloma, urinary bladder, and left ureter of the female mouse (Figures 4F and 5B, inset).

IHC performed on the lung from a female mouse demonstrated that the perivascular and peribronchiolar lymphoid populations were comprised of mixed B and T cell infiltrates, characterized by strong B220 and CD3 immunolabeling, respectively (similar to Figures 1G–I; full images in Figure S1G and H). CD4 and CD8 positive T cells were also detected in association with the peribronchiolovascular inflammation.

ISH was performed to confirm the presence of pulmonary Cm nucleic acid. Occasional strong, specific bronchiolar epithelial cell staining, correlating with the Cm-positive IHC immunolabeling described above, was detected in both the male and female mice (similar to Figure 1F; full image in Figure S1I).

Discussion

We described herein the first cases of Cm-associated clinical disease in mice that were not intentionally exposed to the bacterium since the initial discovery of Cm about 80 y ago.

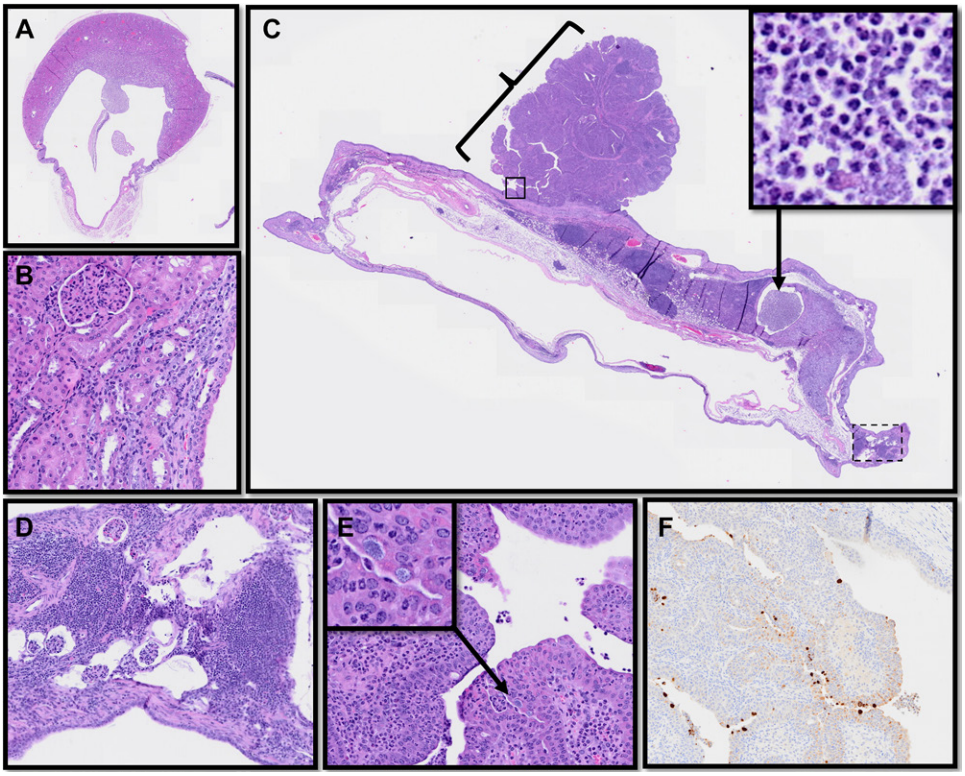

Figure 4. Bilateral hydronephrosis, and Cm-associated unilateral urothelial papilloma, kidneys, female *STAT1*KO mouse. (A) Moderate hydronephrosis with locally extensive parenchymal atrophy, right kidney. HE, subgross. (B) Medullary and cortical tubular degeneration, mild multifocal interstitial nephritis, right kidney. HE, 10×. (C) Severe pyonephritis (neutrophilic inflammation depicted in inset. HE, 10×) with diffuse parenchymal atrophy and urothelial papilloma arising from renal pelvis (bracket), right kidney. HE, subgross. (D) Severe multifocal to coalescing pyonephritis and parenchymal atrophy, indicated by dashed box in C, left kidney. HE, 5×. (E) Severe multifocal to coalescing inflammation and intraurothelial Cm inclusions (boxed area from C), seen only in the urothelium of the papilloma (higher magnification inset); normal urothelial cells without Cm inclusions at top right. Urothelial papilloma; left kidney. HE, 10×. (F) Cm signal in urothelial cells lining the urothelial papilloma, with no signal seen in the normal urothelial cells at top right, left kidney. IHC for Cm MOMP, 10×.

Subsequent to its initial discovery, clinical disease and pathology have only been described in association with experimental infections that used high infectious doses of Cm, or in NSG mice that were intentionally exposed to Cm-shedding mice.[10,13,28,29,38] The NSG mice developed weight loss, lethargy, hunched posture, and dyspnea.[28,38] Their lungs demonstrated either bronchointerstitial pneumonia with occasional intraepithelial chlamydial inclusions or bronchiolitis with similar inclusions. Additional lesions in these mice included neutrophilic rhinitis with intraepithelial Cm inclusions, otitis media, and typhlocolitis.[28,38] One mouse also had urogenital tract involvement that included vaginitis, cervicitis, endometritis, endometrial gland ectasia, and salpingitis with intraepithelial Cm inclusions.[38] Although some overlap was seen in the clinical signs and histopathology of the NSG cohort and the 2 GEM strains described in this report, novel and unexpected lesions were also seen, especially in the urogenital tract of the latter.

The Cm-infected *Il12rb2*KO mice were clinically affected and exhibited a bronchopneumonia or bronchiolitis and multifocal Cm inclusions in surface epithelial cells in the small intestine

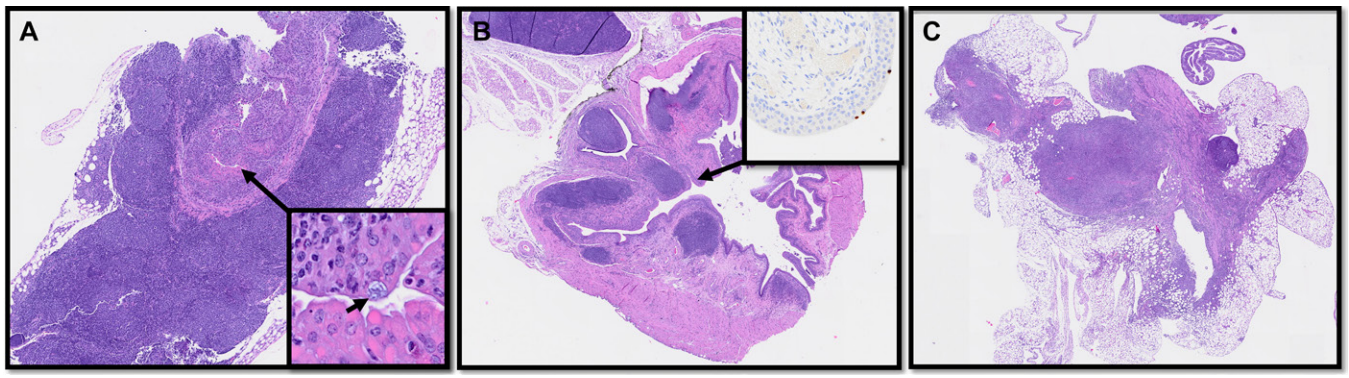

Figure 5. Urogenital lesions, bladder and female reproductive tract, female *STAT1*KO mouse. (A) Severe multifocal to coalescing ureteritis with intraurothelial Cm inclusions and hyaline droplets; higher magnification inset with Cm inclusion (arrow, 10×). Left ureter. HE, subgross. (B) Severe, diffuse cystitis with occasional intraurothelial Cm inclusions (IHC for Cm MOMP; inset, 20×), urothelial cell necrosis, and adjacent lymphoid follicular hyperplasia. Bladder. HE, subgross. (C) Severe ovarian parenchymal atrophy with multifocal to coalescing periovarian steatitis and myositis. Left ovary. HE, subgross.

and colon. The pulmonary pathology seen in these cases shared some similarities to what has been observed in Il12KO mice infected with *C. trachomatis* after intranasal inoculation.[25] One study reported that neutrophils were the most frequent leukocytic cell infiltrate in areas with bronchopneumonia at day 10 after inoculation.[25] In our experience, the difference in cellular infiltrates between this study and the cases presented in the earlier report is likely due to the route of inoculation, infectious dose, and the postinfection duration. Pulmonary histopathology and IHC revealed that mononuclear leukocytic cell infiltrates, including lymphocytes (B and T cells) and macrophages, were frequently associated with pulmonary lesions in clinically affected *Il12rb2*KO mice. Furthermore, while these mice have some deficiency in Th1 response (further described below), the presence of both CD4+ and CD8+ T cells suggests that the Cm infection elicited both Th1 and Th2 responses in the lungs; this was also seen in the *STAT1*KO mice. The thymic hypoplasia we observed likely indicates a negative energy balance (given the low body condition scores) or impaired IL12r signaling that affects T cell development. Further experimental studies would be needed to evaluate the reproducibility of these phenotypes in the lung and thymus. The mouse that presented as moribund could not be further evaluated but presumably was also severely affected by Cm, given our understanding of intracage transmission supported by dirty bedding sentinel testing, observations of spread within research colonies, and ongoing experimental investigations.

The lesions in the *STAT1*KO mice differed considerably from those reported previously in NSG mice and those of the *I112rb2*KO mice described in this report. Cm was more diffusely distributed with unexpected significant lesions in the urogenital tract. Both the male and female *STAT1*KO mice showed some degree of hydronephrosis; a marked suppurative component (pyonephritis) indicative of infection also affected the left kidney of the female mouse. Hydronephrosis is a commonly recognized lesion in mice and has a variety of congenital and acquired etiologies.[37] C57BL/6 mice show a varying incidence of congenital hydronephrosis (for example, 6% in males and 9% in females), whereas it has been seen in up to 100% of male inbred DDD mice.[37] Congenital lesions may be detected in aged mice with milder expression of a genetic trait, and adult mice with unilateral spontaneous hydronephrosis can remain asymptomatic because the unaffected kidney can compensate. Several unique mouse models are also associated with the development of hydronephrosis, including luxate luxoid, short ear, and dominant hemimelia mice, and many transgenic and knockout strains with altered renal physiology.[37] Given that these mice had a C57BL/6 background and were genetically engineered, they may have been genetically predisposed to hydronephrosis; however, the inflammatory lesions seen throughout urogenital tract, often in association with chlamydial inclusions, implicate inflammation associated with Cm as a potential causative factor in the development of the lesions. This idea is supported by the finding that the lesions were worse and bilateral in the female mouse, suggesting the inflammatory process in the lower urinary tract was contributory.

The robust inflammation associated with Cm inclusions in the papilloma and the location of Cm inclusions in the urothelial cells lining the irregular papillary projections indicate the possibility that Cm contributed to the neoplastic lesion. In humans, an association between *C. trachomatis* and urogenital cancers, including ovarian, cervical, kidney, and bladder cancers has been reported.[1,18,30] While definitive causation has not been established between the bacterium and oncogenesis, as with the human papilloma virus (HPV) and cervical cancer, several theoretical mechanisms could predispose tissue to oncogenic transformation. Chronic inflammation has long been associated with carcinogenesis through numerous mechanisms, including free radical production, aberrant tissue repair mediation, and host enzymatic pathways such as the cyclooxygenase system.[1,16,33] Microbes may also directly promote the development of cancer via microbially encoded oncogenes and other factors that alter host cell signaling, including antiapoptotic signals.[1,33] Epidemiologic data indicate that nearly 15% of cancers may be associated with microbial infections, including *Helicobacter pylori*, HPV, and hepatitis B and C viruses.[18,33] *C. trachomatis* and *C. pneumoniae* have been shown to exert antiapoptotic activity through numerous mechanisms, including heat shock proteins.[18,27] The degree of conservation between *Chlamdyia* spp. and demonstration of antiapoptotic activity of Cm in vitro indicate the possibility that Cm may also be associated with neoplastic transformation.[27,31,34]

The male *STAT1*KO mouse showed nonspecific staining in alveolar macrophages and pulmonary epithelial cells with intracytoplasmic eosinophilic crystals and hyaline droplets, consistent with ECP (also known as acidophilic macrophage pneumonia; Figure S1C). This is a common pulmonary lesion in mice, particularly in aged mice on C57BL/6, 129Sv, and outbred Swiss backgrounds.[5,21] ECP is associated with an accumulation of acidophilic crystals both intracellularly (macrophages) and extracellularly (within alveoli and larger airways). Severe cases can lead to morbidity and death.[5,21] ECP can develop spontaneously or as a result of pathologic processes that interfere with appropriate pulmonary function, including pulmonary neoplasia, lymphoproliferative diseases, infections and infestations, or chronic pneumonias.[5,21]

The susceptibility of the 2 GEM strains described in this report to Cm is not surprising. IL-12 is an essential component in both Th1 and Th17 responses to intracellular organisms, with the former required for resolution of Cm infection.[7,24,39] Further, interferon γ (IFNγ) is well known to be crucial in this response, with IFNγ deficient mice demonstrating persistent and sometimes disseminated infections.[7,14,22,32,34] A complex extra- and intracellular pathway leading to the expression of IFNγ begins with extracellular IL-12 binding to the transmembrane IL12 receptor (IL12r). This initiates an intracellular cascade of events involved in the phosphorylation of STAT4, leading to Th1 cell differentiation, monocyte activation, and IFNγ production.[39] The deletion of the IL12r (β 2 gene) in *IL12rb2*KO mice obviously renders them incapable of initiating this pathway, resulting in IFNγ deficiency. *IL12rb2*KO mice have a reduced ability to clear Cm from lung after experimental inoculation; similarly, other mouse lines with impaired IL12 activity have previously been associated with impaired Th1 immune responses and increased susceptibility to pulmonary Cm infection.[7] We also know that IFNγ signals through the JAK-STAT1/STAT1 canonical signaling pathways to activate immune effector genes that encode antimicrobial molecules, phagocytic receptors, chemo- and cytokines, and antigen-presenting cells.[15,22,26] Accordingly, deficiencies in the STAT1 gene in the *STAT1*KO mice render them unable to respond to IFNγ, making them more susceptible to bacterial and viral infection.[11,26] *C. trachomatis*, which shares many genetic similarities to Cm, upregulates phosphorylation of STAT1, and inhibition of that process is associated with increased intracellular chlamydial growth.[17,22] CM001, a clonal isolate purified from Cm Nigg stock, can disseminate to distant anatomic sites (for example, lungs), and can cause death in STAT1KO mice inoculated intravaginally with Cm.[32] Based on our knowledge of *Chlamdia*-related immunology in other species and supported

by case reports in the human literature, we speculate that this mutation would also increase susceptibility to infection with intracellular bacteria such as Cm.[22,32,34,36,42]

Chlamydia is a known cause of infertility in humans, and ample literature describes fertility, gestational, and developmental issues in female and male mice that have been experimentally inoculated with Cm.[6–9,34] Although we did not identify Cm organisms in the reproductive tissues we examined, the breeding issues observed in the STAT1KO mice may be related, at least in part, to Cm infection, as Cm IHC signal was found in the urothelial papilloma and ureter in association with urologic pathology (inflammation, inflammatory tissue hyperplasia, and neoplastic growth) in tissues that abut the reproductive tract. Both local inflammation and systemic inflammation are associated with fertility issues in humans, as inflammation alters hormone production and control (including those associated with ovulation), may lead to anatomic alteration of the genital tract, and affects endometrial receptivity, development, and function.[41,43] Accordingly, a reasonable assumption is that spontaneous Cm infection may affect fertility without directly colonizing the reproductive tract.

In conclusion, this report details the discovery of spontaneous Cm-associated clinical disease and pathology in 2 susceptible GEM strains that do not typically require the specialized husbandry needed to maintain some immunocompromised strains such as NSG. These cases provide as additional examples relevant to considering Cm as an excluded agent in research mouse colonies.

Supplemental Materials

Figure S1. Cm associated bronchopneumonia, lung, *STAT1*KO mice. (A) Male mouse, moderate multifocal peribronchiolar and perivascular bronchointerstitial pneumonia and moderate tracheitis, with lymphoid follicular hyperplasia. HE (subgross). (B) Male mouse, lymphoplasmacytic, histiocytic, and neutrophilic bronchopneumonia noted boxed in A. HE, 20×. (C) Male mouse, nonspecific staining in alveolar macrophages and pulmonary epithelial cells with intracytoplasmic eosinophilic crystals and hyaline droplets (equivocal for Cm, area noted boxed in A). IHC for Cm MOMP, 20×. (D) Female mouse, moderate multifocal peribronchiolar and perivascular bronchointerstitial pneumonia with lymphoid follicular hyperplasia. HE (subgross). (E) Female mouse, intraepithelial inclusions in bronchiolar epithelium noted boxed in D (white arrow) HE, 20×. (F) Female mouse, Cm signal in bronchiolar epithelial cells within inflammatory lesions noted on HE. IHC for Cm MOMP, 20×. (G) Female mouse, peribronchiolar and perivascular T and B cell infiltrates surrounding Cm positive epithelial cells (CD3+ brown, B220+ red). Double staining IHC for CD3 and B220, 10×. (H) Further distinguishing subpopulations within CD3+ cells in prior lesion (CD4+ red, CD8+ brown). Double staining IHC for CD4 and CD8, 10×. (I) Male mouse, Cm nucleic acid in bronchiolar epithelial cell of male mouse (red staining, examples at arrows), confirming infection. ISH for Cm RNA, 20×.

Acknowledgments

We thank Sockie Jiao and the staff of the Laboratory of Comparative Pathology for their technical assistance with IHC and ISH.

Conflict of Interest

The authors have no competing interest to declare.

Funding

MSK Core Facilities are supported by MSK's NCI Cancer Center Support grant P30 CA008748.

References

1. **Alibek K, Karatayeva N, Bekniyazov I.** 2012. The role of infectious agents in urogenital cancers. Infect Agent Cancer **7**:35. https://doi.org/10.1186/1750-9378-7-35.
2. **American Association for Laboratory Animal Services. [Internet].** 2021. Alleviating pain and distress in laboratory animals. [Cited 16 November 2023]. Available at: https://www.aalas.org/about-aalas/position-papers/alleviating-pain-and-distress.
3. **American Association for Laboratory Animal Sciences. [Internet].** 2021. Humane care and use of laboratory animals. [Cited 16 November 2023]. Available at: https://www.aalas.org/about-aalas/positionpapers/humane-care-and-use.
4. **Barron AL, Rank RG, Moses EB.** 1984. Immune response in mice infected in the genital tract with mouse pneumonitis agent (*Chlamydia trachomatis* biovar). Infect Immun **44**:82–85. https://doi.org/10.1128/iai.44.1.82-85.1984.
5. **Barthold SW, Griffey SM, Percy DH.** 2016. Mice: Aging, degenerative, and miscellaneous disorders, p 106–108. In: Barthold SW, Griffey SM, Percy DH**, editors.** Pathology of laboratory rodents and rabbits, 4th ed. Ames (IA): Wiley Blackwell.
6. **Bryan ER, Redgrove KA, Mooney AR, Mihalas BP, Sutherland JM, Carey AJ, Armitage CW, et al.** 2020. Chronic testicular *Chlamydia muridarum* infection impairs mouse fertility and offspring development. Biol Reprod **102**:888–901. https://doi.org/10.1093/biolre/ioz229.
7. **Chen L, Lei L, Zhou Z, He J, Xu S, Lu C, Chen J, et al.** 2013. Contribution of interleukin-12 p35 (IL-12p35) and IL-12p40 to protective immunity and pathology in mice infected with *Chlamydia muridarum*. Infect Immun **81**:2962–2971. https://doi.org/10.1128/IAI.00161-13.
8. **Darville T, Hiltke TJ.** 2010. Pathogenesis of genital tract disease due to *Chlamydia trachomatis*. J Infect Dis **201**:S114–S125. https://doi.org/10.1086/652397.
9. **De La Maza LM, Pal S, Khamesipour A, Peterson EM.** 1994. Intravaginal inoculation of mice with the *Chlamydia trachomatis* mouse pneumonitis biovar results in infertility. Infect Immun **62**:2094–2097. https://doi.org/10.1128/iai.62.5.2094-2097.1994.
10. **Dochez AR, Mills KC, Mulliken B.** 1937. A virus disease of Swiss mice transmissible by intranasal inoculation. Proc Soc Exp Biol Med **36**:683–686. https://doi.org/10.3181/00379727-36-9357.
11. **Durbin JE, Hackenmiller R, Simon MC, Levy DE.** 1996. Targeted disruption of the mouse STAT1 gene results in compromised innate immunity to viral disease. Cell **84**:443–450. https://doi.org/10.1016/S0092-8674(00)81289-1.
12. **Fan Y, Wang S, Wang X.** 1999. *Chlamydia trachomatis* (mouse pneumonitis strain) induces cardiovascular pathology following respiratory tract infection. Infect Immun **67**:6145–6151. https://doi.org/10.1128/IAI.67.11.6145-6151.1999.
13. **Gordon FB, Freeman G, Glampit JM.** 1938. A pneumoniaproducing filtrable agent from stock mice. Proc Soc Exp Biol Med **39**:450–453. https://doi.org/10.3181/00379727-39-10236.
14. **He X, Nair A, Mekasha S, Alroy J, O'Connel CM, Ingalls RR.** 2011. Enhanced virulence of *Chlamydia muridarum* respiratory infections in the absence of TLR2 activation. PLoS One **6**:e20846. https://doi.org/10.1371/journal.pone.0020846.
15. **Hu X, Ivashkiv LB.** 2009. Cross-regulation of signaling and immune responses by IFNy and STAT1. Immunity **31**:539–550. https://doi.org/10.1016/j.immuni.2009.09.002.
16. **Hussain SP, Hofseth LJ, Harris CC.** 2003. Radical causes of cancer. Nat Rev Cancer **3**:276–285. https://doi.org/10.1038/nrc1046.
17. **Ibana JA, Sherchand SP, Fontanilla FL, Nagamatsu T, Schust DJ, Quayle AJ, Aiyar A.** 2018. *Chlamydia trachomatis*-infected cells and uninfected-bystander cells exhibit diametrically opposed responses to interferon gamma. Sci Rep **8**:8476. https://doi.org/10.1038/s41598-018-26765-y.
18. **Idahl A, Lundin E, Jurstrand M, Kumlin U, Elgh F, Ohlson N, Ottander U.** 2011. *Chlamydia trachomatis* and *Mycoplasma genitalium* plasma antibodies in relation to epithelial ovarian tumors. Infect Dis Obstet Gynecol **2011**:824627. https://doi.org/10.1155/2011/824627.
19. **Institute for Laboratory Animal Research.** 2011. Guide for the care and use of laboratory animals, 8th ed. Washington (DC): The National Academies Press. Available at: https://nap.nationalacademies.org/catalog/12910/guide-for-the-care-and-use-of-laboratory-animals-eighth.

20. **Jupelli M, Selby DM, Guentzel MN, Chambers JP, Forsthuber TG, Zhong G, Murthy AK, et al.** 2010. The contribution of interleukin-12/interferon-gamma axis in protection against neonatal pulmonary *Chlamydia muridarum* challenge. J Interferon Cytokine Res **30**:407–415. https://doi.org/10.1089/jir.2009.0083.
21. **Klug JJ, Synder JM.** 2020. Eosinophilic crystalline pneumonia, an age-related lesion in mice. Aging Pathobiol Ther **2**:232–233. https://doi.org/10.31491/APT.2020.12.047.
22. **Lad SP, Fukuda EY, Li J, de la Maza LM, Li E.** 2005. Up-regulation of the JAK/STAT1 signal pathway during *Chlamydia trachomatis* infection. J Immunol **174**:7186–7193. https://doi.org/10.4049/jimmunol.174.11.7186.
23. **Lipman NS, Homberger FR.** 2003. Rodent quality assurance testing: Use of sentinel animal systems. Lab Anim (NY) **32**:36–43. https://doi.org/10.1038/laban0503-36.
24. **Lu H, Shen C, Brunham RC.** 2000. *Chlamydia trachomatis* infection of epithelial cells induces the activation of caspase-1 and release of mature IL-18. J Immunol **165**:1463–1469. https://doi.org/10.4049/jimmunol.165.3.1463.
25. **Lu H, Yang X, Takeda K, Zhang D, Fan Y, Luo M, Shen C, Wang S, Akira S, Brunham RC.** 2000. *Chlamydia trachomatis* mouse pneumonitis lung infection in IL-18 and IL-12 knockout mice: IL-12 is dominant over IL-18 for protective immunity. Mol Med **6**:604–612. https://doi.org/10.1007/BF03401798.
26. **Meraz MA, White JM, Sheehan KC, Bach EA, Rodig SJ, Dighe AS, Kaplan DH, et al.** 1996. Targeted disruption of the Stat1 gene in mice reveals unexpected physiologic specificity in the JAK-STAT signaling pathway. Cell **84**:431–442. https://doi.org/10.1016/S0092-8674(00)81288-X.
27. **Messinger JE, Nelton E, Feeney C, Gondek DC.** 2015. Chlamydia infection across host species boundaries promotes distinct sets of transcribed anti-apoptotic factors. Front Cell Infect Microbiol **5**:96. https://doi.org/10.3389/fcimb.2015.00096.
28. **Mishkin N, Ricart Arbona RJ, Carrasco SE, Lawton S, Henderson KS, Momtsios P, Sigar IM, et al.** 2022. Reemergence of the murine bacterial pathogen *Chlamydia muridarum* in research mouse colonies. Comp Med **72**:230–242. https://doi.org/10.30802/AALAS-CM-22-000045.
29. **Nigg C, Eaton MD.** 1944. Isolation from normal mice of a pneumotropic virus which forms elementary bodies. J Exp Med **79**:497–510. https://doi.org/10.1084/jem.79.5.497.
30. **Paavonen J.** 2001. *Chlamydia trachomatis* and cancer. Sex Transm Infect **77**:154–156. https://doi.org/10.1136/sti.77.3.154.
31. **Perfettini JL, Darville T, Dautry-Varsat A, Rank RG, Ojcius DM.** 2002. Inhibition of apoptosis by gamma interferon in cells and mice infected with *Chlamydia muridarum* (the mouse pneumonitis strain of *Chlamydia trachomatis*). Infect Immun **70**:2559–2565. https://doi.org/10.1128/IAI.70.5.2559-2565.2002.
32. **Poston TB, O'Connell CM, Girardi J, Sullivan JE, Nagarajan UM, Marinov A, Scurlock AM, et al.** 2018. T cell-independent gamma interferon and B cells cooperate to prevent mortality associated with disseminated *Chlamydia muridarum* genital tract infection. Infect Immun **86**:e00143-18. https://doi.org/10.1128/IAI.00143-18.
33. **Rakoff-Nahoum S.** 2006. Why cancer and inflammation? Yale J Biol Med **79**:123–130.
34. **Rank R.** 2007. Chlamydial diseases. p 326–344. In: Fox JG, Davisson MT, Quimby FW, Barthold SW, Newcomer CE, Smith AL, **editors.** The mouse in biomedical research, vol **2**. Burlington (MA): Elsevier.
35. **Rank RG, Soderberg LSF, Barron AL.** 1985. Chronic chlamydial genital infection in congenitally athymic nude mice. Infect Immun **48**:847–849. https://doi.org/10.1128/iai.48.3.847-849.1985.
36. **Rothfuchs AG, Trumstedt C, Mattei F, Schiavoni G, Hidmark A, Wigzell H, Rottenberg ME.** 2006. STAT1 regulates IFN-αβ- and IFN-γ-dependent control of infection with *Chlamydia pneumoniae* by nonhemopoietic cells. J Immunol **176**:6982–6990. https://doi.org/10.4049/jimmunol.176.11.6982.
37. **Springer DA, Allen M, Hoffman V, Brinster L, Starost MF, Bryant M, Eckhaus M.** 2014. Investigation and identification of etiologies involved in the development of acquired hydronephrosis in aged laboratory mice with the use of high-frequency ultrasound imaging. Pathobiol Aging Age Relat Dis **4**:1. https://doi.org/10.3402/pba.v4.24932.
38. **St Jean SC, Ricart Arbona RJ, Mishkin N, Monette S, Wipf JRK, Henderson KS, Cheleuitte-Nieves C, et al.** 2024. *Chlamydia muridarum* infection causes bronchointerstitial pneumonia in NOD.Cg-*Prkdc*^{scid}*Il2rg*^{tm1Wjl}/SzJ (NSG) mice. Vet Pathol **61**:145–156. https://doi.org/10.1177/03009858231183907.
39. **Tait Wojno ED, Hunter CA, Stumhofer JS.** 2019. The immunobiology of the interleukin-12 family: Room for discovery. Immunity **50**:851–870. https://doi.org/10.1016/j.immuni.2019.03.011.
40. **Thurlow RW, Arriola R, Soll CE, Lipman NS.** 2007. Evaluation of a flash disinfection process for surface decontamination of gamma-irradiated feed packaging. J Am Assoc Lab Anim Sci **46**:46–49.
41. **Ullman-Cullere MH, Foltz CJ.** 1999. Body condition scoring: A rapid and accurate method for assessing health status in mice. Lab Anim Sci **49**:319–323.
42. **Vairo D, Tassone L, Tabellini G, Tamassia N, Gasperini S, Bazzoni F, Plebani A, et al.** 2011. Severe impairment of IFNγ and IFNα responses in cells of a patient with a novel STAT1 splicing mutation. Blood **118**:1806–1817. https://doi.org/10.1182/blood-2011-01-330571.
43. **Weiss G, Goldsmith LT, Taylor RN, Bellet D, Taylor RN.** 2009. Inflammation in reproductive disorders. Reprod Sci **16**:216–229. https://doi.org/10.1177/1933719108330087.
44. **Wu C, Wang X, Gadina M, O'Shea JJ, Presky DH, Magram J.** 2000. IL-12 receptor B2 (IL-12RB2)-deficient mice are defective in IL-12-mediated signaling despite the presence of high affinity IL-12 binding sites. J Immunol **165**:6221–6228. https://doi.org/10.4049/jimmunol.165.11.6221.
45. **Yeruva L, Spencer N, Bowlin AK, Wang Y, Rank RG.** 2013. Chlamydial infection of the gastrointestinal tract: A reservoir for persistent infection. Pathog Dis **68**:88–95. https://doi.org/10.1111/2049-632X.12052.